PRAMANA — journal of physics

Vol. 83, No. 3
September 2014
pp. 413–425

Elastic constants and Debye temperature of wz-AlN and wz-GaN semiconductors under high pressure from first-principles

B P PANDEY[1,*], V KUMAR[2] and EDUARDO MENENDEZ PROUPIN[3]
[1]Department of Electronics & Communication Engineering, GLA University, Mathura 281 406, India
[2]Department of Electronic Engineering, Indian School of Mines, Dhanbad 826 004, India
[3]Departamento de Fisica, Facultad de Ciencias, Universidad de Chile, Santiago, Chile
*Corresponding author. E-mail: pandey.bramha@gmail.com

MS received 20 October 2013; revised 12 January 2014; accepted 28 January 2014
DOI: 10.1007/s12043-014-0785-7; ***e*Publication:** 5 September 2014

Abstract. First-principles calculations were performed to study the elastic stiffness constants (C_{ij}) and Debye temperature (θ_D) of wurzite (wz) AlN and GaN binary semiconductors at high pressure. The lattice constants were calculated from the optimized structure of these materials. The band gaps were calculated at Γ point using local density approximation (LDA) approach. The unit cell volume, lattice parameters, c/a, internal parameter (u), elastic constant (C_{ij}), Debye temperature (θ_D), Hubbard parameter (U) and band gap (E_g) were studied under different pressures. The bulk modulus (B_0), reduced bulk modulus (B_0') and Poisson ratio (υ) were also calculated. The calculated values of these parameters are in fair agreement with the available experimental and reported values.

Keywords. Debye temperature; elastic constants; band gap; first-principles; DFT+U

PACS Nos 61.82.Fk; 63.20.dk; 71.15.Mb; 71.20.−b; 78.55.Cr

1. Introduction

The III–V groups of nitrides have attracted much attention due to their potential applications in the fields of optoelectronics because of their use as wide band gap optical sources, their superhardness properties, uses at high temperature and pressure, high density data storage capacity and high power conversion efficiency [1,2]. Wurtzite AlN and GaN are more stable compared to zinc-blende structures of AlN and GaN [3]. The chemical prototype of wurtzite structure is ZnS with hexagonal structure (B4), Hermann–Mauguin notation of which is P63mc. Moreover, because of their wide band gap and good thermal conductivity, wz-AlN and wz-GaN also have potential applications in high-temperature, high-power electronic devices and others in visible and ultraviolet region by

varying the wide band gap [4,5]. These two are also very prominent binary compounds in extreme conditions of high pressure and temperature. Therefore, experimental and theoretical investigations are of great interest to physicists and researchers. Earlier work [6–8] explored more information with improved accuracy about the characteristics of wz-AlN and wz-GaN. It was found that wz-AlN and wz-GaN were thermodynamically stable at ambient environment, but the structural phase and the thermodynamic stability of wz-AlN and wz-GaN under high temperature and pressure remain uncertain.

In the present work, we have investigated the structural properties, elastic constants and Debye temperature of wz-AlN and wz-GaN at high pressure by using the first-principles plane-wave method in the frame of DFT with local density approximation (LDA). We have also calculated band-gap properties at different pressures, which are underestimated due to intrinsic property of LDA approximation. Band gaps for wz-AlN and wz-GaN have been corrected by using the DFT+U method under the linear response method by estimating the value of U at different pressures. The results obtained are in good agreement with the available experimental results and other reported theoretical methods.

2. Computational methods

First principles total energy calculations were performed using quantum-espresso code [9]. The interaction between ions and valence electrons were described by the USPP method [10] for both the binary semiconductors. The exchange and correlation effects were treated by the local density approximation of Perdew and Zunger [11]. The k mesh was sampled according to a Monkhorst–Pack scheme as 4 4 2 with a spacing of 0.5/Å [12]. The electronic configurations for Al, Ga and N are [Ne]$2s^2 2p^1$, [Ar]$3d^{10}4s^2 4p^1$ and [He]$2s^2 2p^3$, respectively. The valence electrons were taken as 3, 13 and 5, respectively for Al, Ga and N. The $3d^{10}$ electrons were considered as valence electrons to observe the non-localized effect of d shell in Ga atom. The energy cut-off in the plane-wave expansion is 65 Ry and cut-off for charge density is 720 Ry for the wz-AlN and wz-GaN semiconductors. Convergence of relative energies with respect to the k mesh and energy cut-off was found to be better than 1 meV/atom. The cut-off of plane-wave expansion is high for hard pseudopotential of N atom. The equation of state (EoS) was used to determine equilibrium structural properties for wz-AlN and wz-GaN at different pressures. Elastic constants, Debye temperature and band gap were calculated at different pressures.

3. Results and discussion

3.1 *Structural properties*

To calculate the structural properties of wz-AlN and wz-GaN, we have used the local density approximation (LDA) pseudopotential. The graph between total energy and volume are plotted for wz-AlN and wz-GaN in figure 1 to determine the equation of state and to find the equilibrium ($P = 0$, $T = 0$) parameters like lattice constant a, c/a ratio and u. The calculated equilibrium lattice parameters are 5.83 and 5.97 Å, c/a parameters are 1.58 and 1.61, internal u are 0.382 and 0.376 and bulk moduli are 204.6 and 182.5 GPa for wz-AlN and wz-GaN, respectively. The calculated equilibrium lattice parameters are

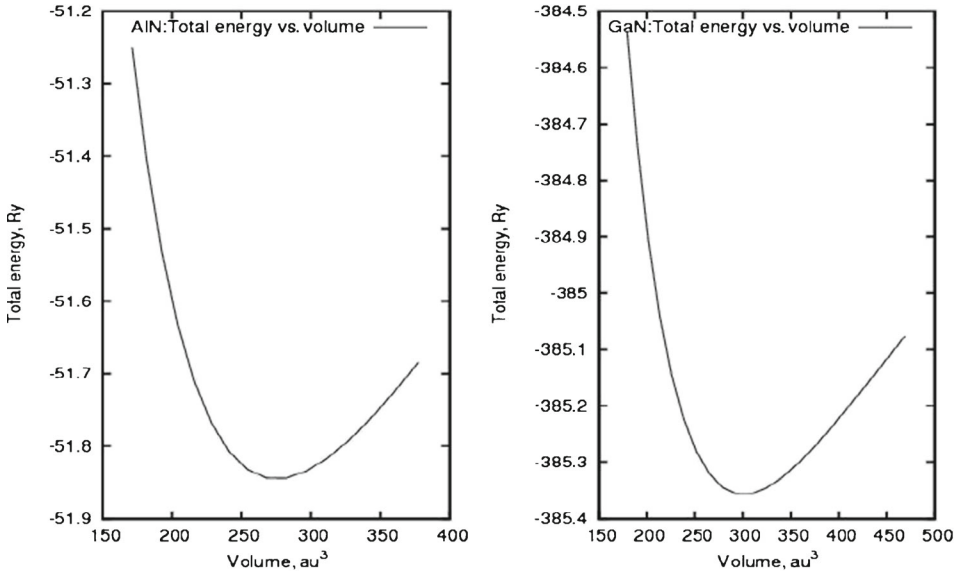

Figure 1. Variation of total energy (Ry) with volume in Bohr (a.u.) for wz-AlN and wz-GaN for obtaining the equilibrium ($P = 0$, $T = 0$) lattice parameters.

underestimated due to the inherent property of LDA pseudopotentials. We have also plotted the graph between volume and pressure for wz-AlN and wz-GaN in figure 2. The obtained equilibrium lattice parameters are compared with available experimental and reported data given in table 1. Structural properties like lattice parameter (a), c/a ratio

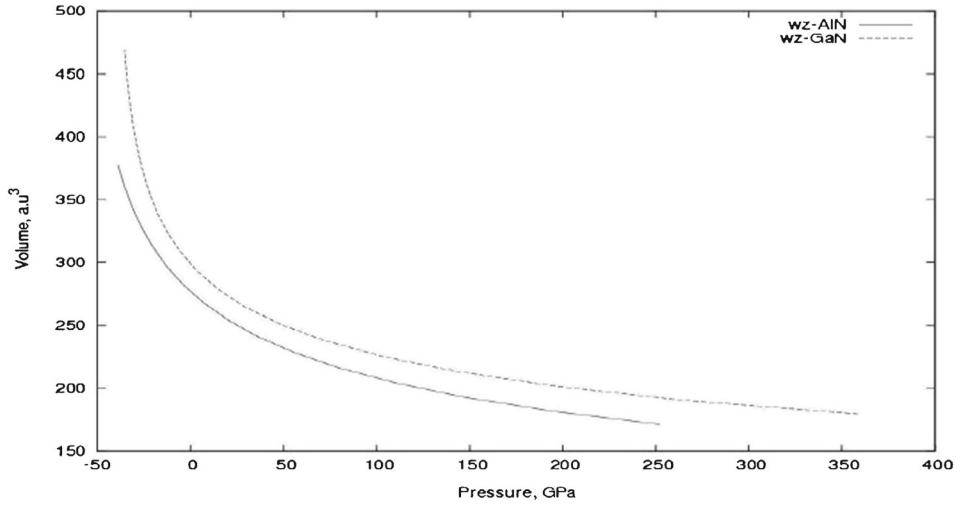

Figure 2. Variation of volume (a.u.^{3}) with pressure (GPa) for wz-AlN and wz-GaN at equilibrium ($P = 0$, $T = 0$) lattice parameters.

Table 1. Lattice constant (a), c/a parameter, internal parameter (u), bulk modulus (B), pressure derivative of bulk modulus (B'), volume (Å^3/atom) and Poisson's ratio (υ) of wz-AlN and wz-GaN semiconductors.

Compound		Lattice constant (Å)	c/a	u	B (GPa)	B'	V_0 (Å^3/atom)	Poisson's ratio (υ)	Debye temperature (θ_D)
This work	wz-AlN	3.084	1.58	0.382	204.6[v], 211[w]	3.46	41.01	0.25091	835.76
	wz-GaN	3.158	1.61	0.376	182.5[v], 203[w]	4.47	44.27	0.26552	521.93
Expt. values	wz-AlN	3.112[a]	1.60[a]		201[d]			0.255°, 0.236[m]	
	wz-GaN	3.189[b]	1.626[b]		180[e]			0.371[p], 0.228[q,r]	600–800[s]
Theoretical values	wz-AlN	3.144[c]	1.605[c]	0.381[c]	194[c], 207[f]			0.257[n]	1025[u]
	wz-GaN	3.146[c]	1.629[c]	0.377[c]	195[c], 202[f]			0.212[l]	867[u], 826[t]

[a]Ref. [41]; [b]Ref. [42]; [c]Ref. [43]; [d]Ref. [20]; [e]Ref. [21]; [f]Ref. [16]; [l]Ref. [27]; [m]Ref. [28]; [n]Ref. [29]; [o]Ref. [30]; [p]Ref. [31]; [q]Ref. [32]; [r]Ref. [33]; [s]Ref. [34]; [t]Ref. [34]; [u]Ref. [35].
[v]Calculated from EOS.
[w]Calculated from elastic constants.

and u have also been calculated at different pressures and plotted in figure 3 for both wz-AlN and wz-GaN. It has been observed that for wz-AlN, the lattice parameter a, and c/a decreases and u increases monotonically with increasing pressure, whereas for wz-GaN, though the lattice parameter a and c/a show the same trend as that are shown by wz-AlN, u displays opposite trend with pressure.

3.2 *Debye temperature (θ_D) calculation using elastic constants*

The Debye temperatures for wz-AlN and wz-GaN are calculated using elastic constants [13], whereas elastic constants are calculated at equilibrium ($P = 0$, $T = 0$) lattice parameter. The stiffness constants are defined as

$$C_{ij} \equiv c_{\alpha\beta\gamma\delta} = \frac{1}{V_0}\frac{\partial^2 E_{\text{total}}}{\partial\varepsilon_{\alpha\beta}\delta\varepsilon_{\gamma\delta}}, \tag{1}$$

where E_{total} and V_0 are the total energy and the equilibrium volume, respectively. $\sigma_{\alpha\beta}$ and $\varepsilon_{\alpha\beta}(\alpha, \beta = x, y, z)$ are the components of the stress and strain tensors respectively. Non-zero and independent elastic stiffness constants of hexagonal crystal structures using Voigt indices' are C_{11}, C_{12}, C_{13}, C_{33}, C_{44} and C_{66} [14]. The general strain tensor matrix is given as $\begin{bmatrix} \varepsilon_{11} & \varepsilon_{12} & \varepsilon_{13} \\ \varepsilon_{21} & \varepsilon_{22} & \varepsilon_{23} \\ \varepsilon_{31} & \varepsilon_{32} & \varepsilon_{33} \end{bmatrix}$. For calculating elastic stiffness constants, C_{11}, C_{12}, C_{13}, C_{33} and C_{44}, we have taken non-zero ε_{11}, $(\varepsilon_{11}, \varepsilon_{22})$, $(\varepsilon_{11}, \varepsilon_{33})$, ε_{33} and $(\varepsilon_{23}, \varepsilon_{32})$, respectively, and other strain tensor components equal to zero in strain tensor matrix. For determining

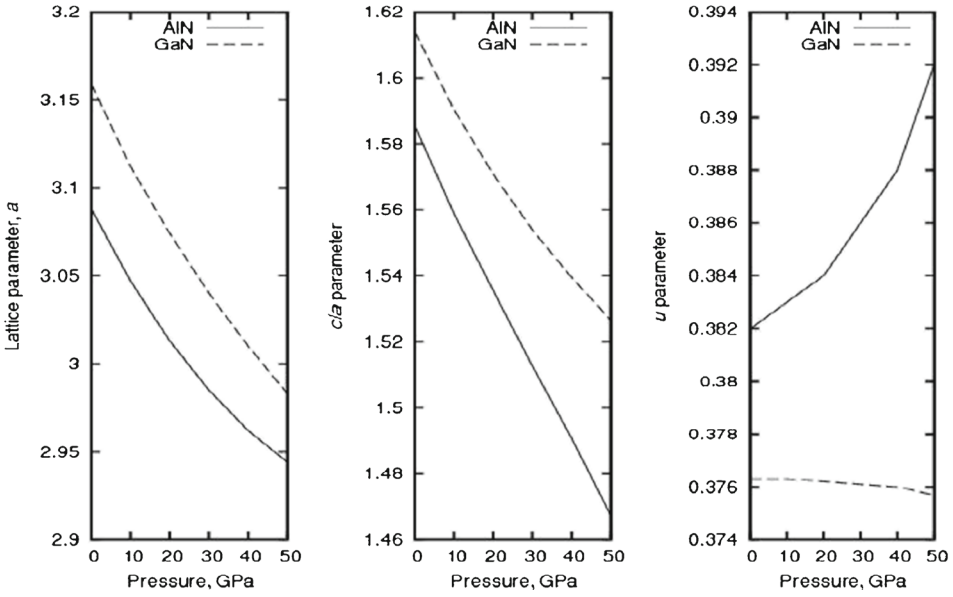

Figure 3. Variations of lattice parameter (a), c/a and u at different pressures are shown for wz-AlN and wz-GaN. All these parameters decrease except u which increases for wz-AlN and slightly decrease for wz-GaN as pressure increases.

the stiffness constant, we have calculated energies of wz-AlN and wz-GaN crystals for the small volume conserving strains using the periodic DFT method. We have fitted the stiffness constants (C_{ij}) to the energy–strain relations, $U(\varepsilon) = 0.5C_{11}\varepsilon_{xx}^2$, $U(\varepsilon) = (C_{11} + C_{12})\varepsilon_{xx}^2$, $U(\varepsilon) = 0.5(C_{11} + C_{33} + 2C_{13})\varepsilon_{xx}^2$, $U(\varepsilon) = 0.5C_{33}\varepsilon_{xx}^2$ and $U(\varepsilon) = 2C_{44}\varepsilon_{xx}^2$ for calculating C_{11}, C_{12}, C_{13}, C_{33} and C_{44}, respectively, and $C_{66} = 0.5(C_{11}-C_{12})$, where $\varepsilon_{xx}(x = 1, 2, 3)$ are the strain tensor components and $U(\varepsilon) = E_{\text{total}}(\varepsilon)/V_0$ is the total energy per unit volume. We have applied seven independent small strains (ε_{xx}), 0, ± 0.015, ± 0.010, ± 0.005. The total energy, $E_{\text{total}}(\varepsilon)$ after applying small strains, were fitted to the polynomial equation

$$E_{\text{total}}(\varepsilon) = V_0 U(\varepsilon) = A_0 + A_1\varepsilon + A_2\varepsilon^2 + A_3\varepsilon^3, \tag{2}$$

where A_0, A_1, A_2 and A_3 are the fitting parameters. A_1 corrects inaccuracies in the variable cell optimization, and A_3 corrects the anharmonic term [15]. The third term A_2 is important for calculating stiffness constants where $A_2/V_0 = C_{11}/2$ for strain ε_{11}, $(C_{11}+ C_{12})$ for strain $(\varepsilon_{11} = \varepsilon_{22})$, $(C_{11}+ C_{33}+ 2C_{13})/2$ for strain $(\varepsilon_{11} = \varepsilon_{33})$, $C_{33}/2$ for strain ε_{33} and $2C_{44}$ for strain $(\varepsilon_{23} = \varepsilon_{32})$. The calculated stiffness constants are given in table 2. The obtained values of stiffness constants for wz-AlN and wz-GaN are in good agreement with the values reported by other theoretical works and available experimental data. The calculated results are also plotted in figures 4 and 5 at different pressures. The theoretical [16–19] values of stiffness constants for wz-AlN and wz-GaN are overestimated when compared to the experimental values [20,21]. The Debye temperature (θ_{D}) defined as a measure of the cut-off frequency by $\theta_{\text{D}} = \hbar\omega_{\text{D}}/k_{\text{B}}$, is then proportional to the Debye sound velocity, v_{D}:

$$\theta_{\text{D}} = \frac{\hbar}{k_{\text{B}}}\left(\frac{6\pi^2 N}{V}\right)^{1/3} v_{\text{D}} \tag{3}$$

and

$$v_{\text{D}} = k(\upsilon)\sqrt{\frac{B}{\rho}}. \tag{4}$$

The bulk modulus (B) and Poisson ratio υ of a polycrystalline material are estimated from the single crystal elastic constants by the Voigt–Reuss–Hill (VRH) approximation [22]. θ_{D} and $k(\upsilon)$ can be given in more usable format in terms of atomic weight M and Poisson ratio υ as

$$\theta_{\text{D}} = k(\upsilon)\frac{\hbar}{k_{\text{B}}}\left(\frac{6\pi^2\rho}{M}\right)^{1/3}\sqrt{\frac{B}{\rho}} \tag{5}$$

and

$$k(\upsilon) = \left[\frac{1}{3}\left[\left[\frac{1+\upsilon}{3\,(1-\upsilon)}\right]^{3/2} + 2\left[\frac{2\,(1+\upsilon)}{3\,(1-2\upsilon)}\right]^{3/2}\right]\right]^{-1/3}. \tag{6}$$

θ_{D} can be further rewritten as

$$\theta_{\text{D}} = k(\upsilon)\frac{\hbar}{k_{\text{B}}}\left(48\pi^5\right)^{1/6}\sqrt{\frac{r_0\beta}{M}}. \tag{7}$$

Table 2. Calculated elastic stiffness constants, C_{ij} (in GPa) for wz-AlN and wz-GaN semiconductors under different pressures.

Elastic constants		Calculated elastic stiffness constants C_{ij} (in GPa) under different pressures							
		At 0 GPa			This work at				
		This work	Expt. values	Reported values	10 GPa	20 GPa	30 GPa	40 GPa	50 GPa
C_{11}	wz-AlN	401	345[d]	345[d], 396[f], 411[g], 398[k]	441.02	476.84	509.7	540.73	568.44
	wz-GaN	366	374[e]	367[f], 365[h], 377[i], 390[j]	410.28	448.16	484.78	514.42	545.08
C_{12}	wz-AlN	143	125[d]	125[d], 137[f], 149[g], 140[k]	173.56	204.01	233.91	264.19	296.31
	wz-GaN	140	106[e]	135[f,h], 160[i], 145[j]	174.26	205.54	237.3	267.03	297.42
C_{13}	wz-AlN	112	120[d]	120[d], 108[f], 99[g], 127[k]	141.35	170.97	201.79	233.99	269.13
	wz-GaN	100	70[e]	103[f], 114[h], 114[i], 106[j]	129.58	158.66	188.36	218.91	246.72
C_{33}	wz-AlN	369	395[d]	395[d], 373[f], 389[g], 382[k]	392.99	409.39	415.87	412.45	390.77
	wz-GaN	411	379[e]	405[f], 381[h], 209[i], 398[j]	464.39	507.96	548.35	584.25	622.75
C_{44}	wz-AlN	118	118[d]	118[d], 116[f], 125[g], 96[k]	125.33	132.51	140	148.38	158.44
	wz-GaN	96	101[e]	95[f], 109[h], 81.4[i], 105[j]	100.88	103.65	105.99	106.41	107.62

[d]Ref. [20]; [e]Ref. [21]; [f]Ref. [16]; [g]Ref. [23]; [h]Ref. [24]; [i]Ref. [25]; [j]Ref. [26]; [k]Ref. [17].

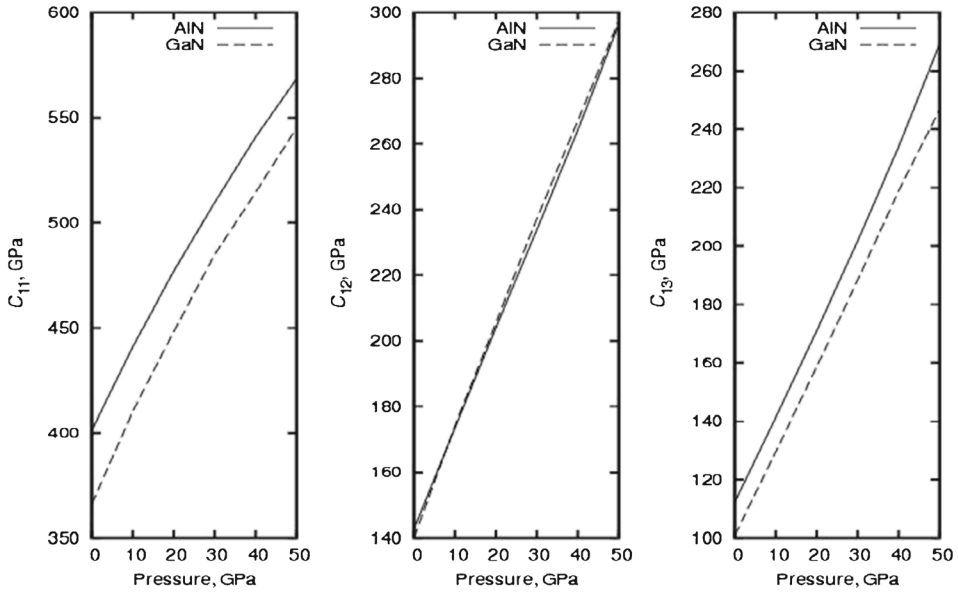

Figure 4. Elastic constants C_{11}, C_{12} and C_{13} are shown at different pressures for wz-AlN and wz-GaN. For wz-AlN, C_{11} and C_{13} are higher when compared to wz-GaN and similar for C_{12}.

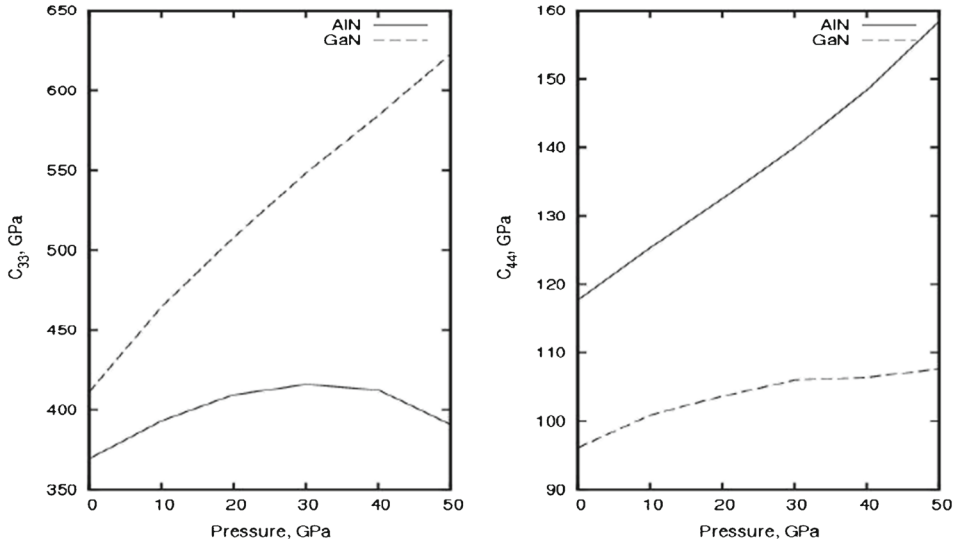

Figure 5. Elastic constants C_{33} and C_{44} are shown at different pressures for wz-AlN and wz-GaN. C_{33} increases linearly for wz-GaN but decreases for wz-AlN as pressure increases and C_{44} for wz-AlN is higher when compared to wz-GaN.

In this expression, r_0 is the equilibrium Wigner–Seitz radius, which is defined as $4\pi r_0^3/3 = V_0/N = M/\rho$, where V_0 and N are equilibrium volume and number of atoms per unit cell, respectively. The Debye temperature (θ_D) obtained from the elastic constants using eq. (7) is compared with the available experimental values which are in good agreement with some allowable error given in table 1 and plotted in figure 6. It is observed that Debye temperature (θ_D) increases slightly as pressure increases till 40 GPa and unstable above 40 GPa due to the instability of wz-AlN and wz-GaN.

3.3 *Band-gap correction for wz-AlN and wz-GaN using DFT+U*

The energy band gaps of wz-AlN and wz-GaN structures are calculated using LDA approach. To correct the energy band gap, LDA+U is incorporated in LDA pseudopotential to calculate the more accurate electronic property of the wz-AlN and wz-GaN binary semiconductors. LDA+U method is first introduced by Anisimov and co-workers [36] for studying strongly correlated compounds with much improved result compared to LSDA, GGA and LDA results. LDA+U is Hamiltonian correction, which is responsible for Hubbard interaction (E_{HUB}), and is given as

$$E_{LDA+U}[n(r)] = E_{LDA}[n(r)] + E_{HUB}\left[n_m^{I\sigma}\right] - E_{DC}\left[n^{I\sigma}\right], \tag{8}$$

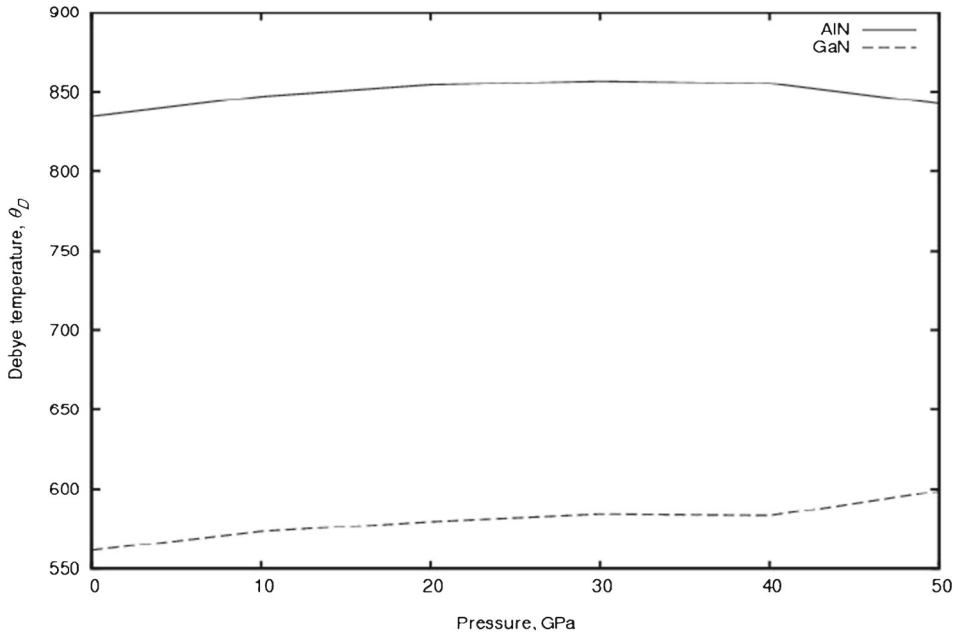

Figure 6. Debye temperature vs. pressure is shown and Debye temperature for wz-AlN and wz-GaN are increased from equilibrium.

where $n(r)$ is the electronic density and $n_m^{I\sigma}$ is the atomic orbital occupations for the atom I experiencing the Hubbard term. The last term in eq. (8) is used to avoid double counting of the interactions contained in both E_{HUB} and E_{LDA}. Each component on the right-hand side of eq. (8) is well described in refs [36–38]. In practical calculation of LDA+U, two parameters U and J are described as screen Couloumb and exchange interactions by Anisimov and co-workers in LMTO calculations, using supercells, revealed that the occupations of localized orbital are compelled to delocalize one atom orbital. A simplified rotationally invariant technique and U_{eff} are proposed by Matteo Cococioni and Stefano de Gironcoli [39]. The U_{eff} parameter can be represented as U–J. For practical calculations, constraining the localized orbital occupations are easier by Legendre transform in which independent variables α_I's are used. The α_I is added or subtracted to the single-particle potential. Therefore, the density response functions of the system, with respect to these localized perturbations are given [39] as

$$X_{IJ} = \frac{\partial^2 E}{\partial a_I \partial a_J} = \frac{\partial n_I}{\partial a_J}, \tag{9a}$$

$$X^0_{IJ} = \frac{\partial^2 E^{KS}}{\partial a_I^{KS} \partial a_J^{KS}} = \frac{\partial n_I}{\partial a_J^{KS}}. \tag{9b}$$

Using the above density response functions, the effective interaction parameter, U_{eff}, associated with I atoms can be calculated as

$$U_{\mathrm{eff}} = \frac{+\partial a_I^{KS}}{\partial q_I} - \frac{\partial a_I}{\partial q_I} = \left(X_0^{-1} - X^{-1}\right)_{II}. \tag{10}$$

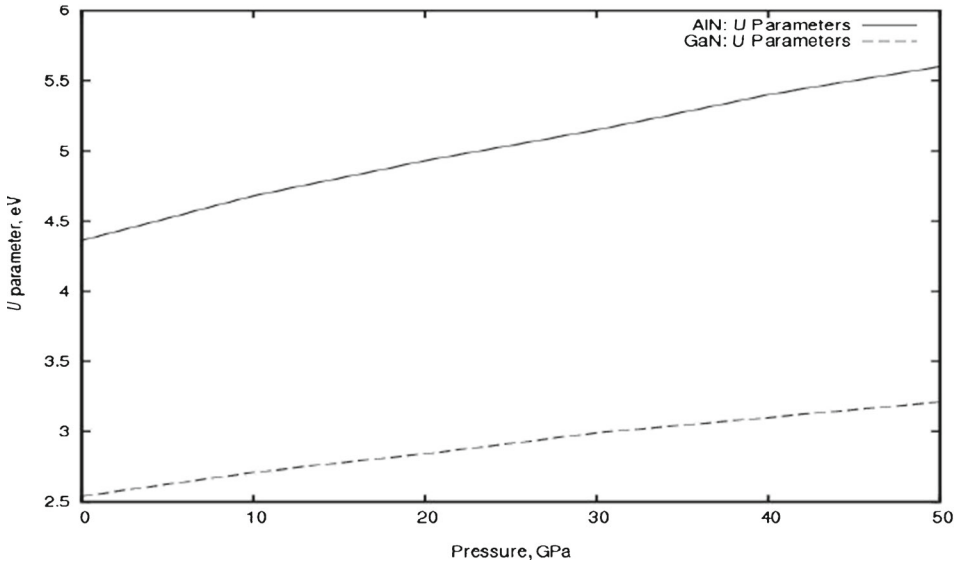

Figure 7. Hubbard U parameter vs. pressure for wz-AlN and wz-GaN.

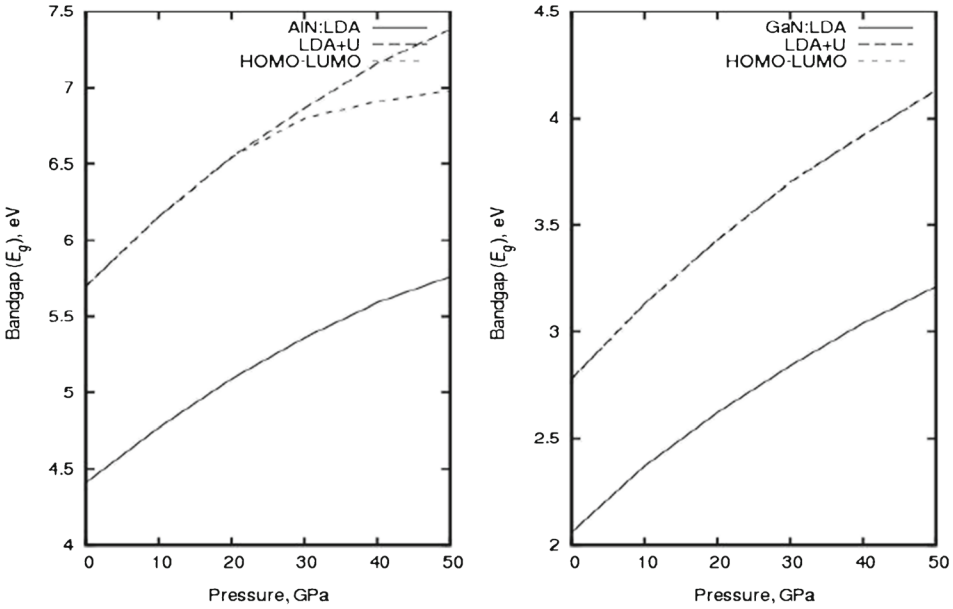

Figure 8. Band-gap variation vs. pressure for wz-AlN and wz-GaN. AlN: LDA band gap with LDA pseudopotential, LDA+U band gap with LDA+U correction and HOMO–LUMO effect has been observed after 20 GPa in wz-AlN but HOMO-LUMO splitting in wz-GaN has not been observed till 50 GPa.

The density response functions, eqs (9a), (9b), are needed in eq. (10) to evaluate the unconstrained system ($\alpha_I = 0$) for all sites in the supercell and to provide some constrained value to system ($\alpha_I =$ varying near to zero) in positive and negative values. The Hubbard parameters U, calculated for a single cell at different pressures and plotted in figure 7, reveal that as pressures increases, U increases linearly with respect to pressures for both wz-AlN and wz-GaN. Band gap was calculated with and without U. Band gaps values are lower due to the intrinsic properties of LDA pseudopotentials against the experimental values. To correct the band gap, U was incorporated with LDA and partially filled p state of N atom was perturbed by applying U for both wz-AlN and wz-GaN. Band gap with DFT+U were also calculated at different pressures. Highest occupied molecular orbital (HOMO) and lowest unoccupied molecular orbital (LUMO) band effects were observed above 20 GPa in wz-AlN, but not in wz-GaN as shown in figure 8. The phase transition in wz-AlN was occurred above 20 GPa [40]. The results of the present work was compared with the available experimental [20,21,41,42] and theoretical data [16,23,24,43].

4. Conclusions

In summary, we have performed first-principles calculations for wz-AlN and wz-GaN and determined the equilibrium lattice parameters a and c/a, and u. The variation of structural parameters as a function of pressure was also investigated. The calculation of

Debye temperature using elastic constants and variation of these quantities as a function of pressure were investigated. The band gap values, calculated at different pressures are lesser against the experimental values due to the intrinsic property of LDA pseudopotentials. Band gaps at various pressures were corrected by estimating the value of U using the DFT+U approach under the linear response method for wz-AlN and wz-GaN. All the results obtained are consistent with the experimental and reported results from other workers.

References

[1] I Vurgaftman, J R Meyer and L R Ram-Mohan, *J. Appl. Phys.* **89**, 5815 (2001)
[2] G Chris, Van de Walle and Jorg Neugebauer, *J. Appl. Phys.* **95**, 3851 (2004)
[3] T Schupp, K Lischka and D J As, *J. Crystal Growth* **312**, 1500 (2010)
[4] Hao Yan-Jun, Cheng Yan, Wang Yan-Ju and Chen Xiang-Rong, *Chin. Phys. Soc.* **16(1)**, 217 (2007)
[5] G Will and P G Perkins, *Diamond Relat. Mater.* **10**, 2010 (2001)
[6] S Strite and H Morkoc, *J. Vac. Sci. Technol. B* **10**, 1237 (1992)
[7] O Ambacher, *J. Phys. D: Appl. Phys.* **31**, 2653 (1998)
[8] Hadis Morkoc, *Handbook of nitride semiconductors and devices* (Wiley-VCH Verlag GmbH & Co., KGaA, Weinheim, 2008) ISBN: 978-3-527-40837-5, Vol. 1, pp. 1–1311
[9] P Giannozzi *et al*, *J. Phys.: Condens. Matter* **21**, 395502 (2009)
[10] D Vanderbilt, *Phys. Rev. B* **41**, 7892 (1990)
[11] J P Perdew and A Zunger, *Phys. Rev. B* **23**, 5048 (1981)
[12] H J Monkhorst and J D Pack, *Phys. Rev. B* **13**, 5188 (1976)
[13] Q Chen and B Sundman, *Acta Mater.* **49**, 947 (2001)
[14] E Dieulesaint and D Royer, *Elastic waves in solids* (Wiley, Chichester, 1980)
[15] E Menendez-Proupin, S Cervantes-Rodriguez, R Osorio-Pulgar, M Franco-Cisterna, H Camacho-Montes and M E Fuentes, *J. Mech. Behav. Biomed. Mater* **4**, 1011 (2011)
[16] A F Wright, *J. Appl. Phys.* **82**, 2833 (1997)
[17] K Kim, W R L Lambrecht and B Segall, *Phys. Rev. B* **53**, 16310 (1996)
[18] J M Wagner and F Bechstedt, *Phys. Rev. B* **66**, 115202 (2002)
[19] D Gerlich, S L Dole and G A Slack, *J. Phys. Chem. Solids* **47**, 437 (1986)
[20] K Tsubouchi, K Sugai and N Mikoshiba, *IEEE Ultrason. Symp.* **1**, 375 (1981)
[21] Y Takagi, M Ahart, T Azuhato, T Sota, K Suzuki and S Nakamura, *Physica B* **219**, 547 (1996)
[22] R Meister and L Peselnick, *J. Appl. Phys.* **37**, 4121 (1966)
[23] L E McNeil, M Grimsditch and R H French, *J. Am. Ceram. Soc.* **76**, 1132 (1993)
[24] M Yamaguchi, T Yagi, T Azuhata, T Sota, K Suzuki, S Chichibu and S Nakamura, *J. Phys.: Condens. Matter* **9**, 241 (1997)
[25] R B Schwarz, K Khachaturyan and E R Weber, *Appl. Phys. Lett.* **70**, 1122 (1997)
[26] A Polian, M Grimsditch and I Grzegory, *J. Appl. Phys.* **79**, 3343 (1996)
[27] K Shimada, T Sota and K Suzuki, *J. Appl. Phys.* **84**, 4951 (1998)
[28] K Kim, W R L Lambrecht and B Segall, *Phys. Rev. B* **53**, 16310 (1996)
[29] R Kato and J Hama, *J. Phys.: Condens. Matter* **6**, 7617 (1994)
[30] K Tsubouchi and N Mikoshiba, *IEEE Trans. Sonics Ultrason.* **SU-32**, 634 (1985)
[31] A Savastenko and A U Sheleg, *Phys. Status Solidi A* **48**, K135 (1978)
[32] M Yamaguchi, T Yagi, T Azuhata, T Sota, K Suzuki, S Chichibu and S Nakamura, *J. Phys.: Condens. Matter* **9**, 241 (1997)

[33] M Yamaguchi, T Yagi, T Sota, T Deguchi, K Shimada and S Nakamura, *J. Appl. Phys.* **85**, 8502 (1999)
[34] J Petalas, S Logothetidis and S Boultadakis, *Phys. Rev. B* **52**, 8082 (1995)
[35] D Sedmidubsk, J Leitner, P Svoboda, Z Soferand and J Macháek, *J. Thermal Anal. Calorimetry* **95(2)**, 403 (2009)
[36] V I Anisimov, J Zaanen and O K Andersen, *Phys. Rev. B* **44**, 943 (1991)
[37] V I Anisimov, I V Solovyev, M A Korotin, M T Czyzyk and G A Sawatzky, *Phys. Rev. B* **48**, 16929 (1993)
[38] I V Solovyev, P H Dederichs and V I Anisimov, *Phys. Rev. B* **50**, 16861 (1994)
[39] Matteo Cococcioni and Stefano de Gironcoli, *Phys. Rev. B* **71**, 035105 (2005)
[40] T Mashima *et al*, *J. Appl. Phys.* **86**, 6710 (1999)
[41] W M Yim and R J Paff, *J. Appl. Phys.* **45**, 1456 (1974)
[42] H P Maruska and J J Tietjen, *Appl. Phys. Lett.* **15**, 327 (1986)
[43] K Miwa and A Fukumoto, *Phys. Rev. B* **48**, 7897 (1993)